Atmospheric Environment 132 (2016) 111–122

Contents lists available at ScienceDirect

Atmospheric Environment

journal homepage: www.elsevier.com/locate/atmosenv

Spatio-temporal variability of aerosols over East China inferred by merged visibility-GEOS-Chem aerosol optical depth

Jintai Lin*, Jing Li

Laboratory for Climate and Ocean-Atmosphere Studies, Department of Atmospheric and Oceanic Sciences, School of Physics, Peking University, Beijing 100871, China

HIGHLIGHTS

- A gridded multi-year AOD dataset by merging visibility observations and model simulations.
- The merged AOD dataset is spatially and temporally consistent with MODIS and ground networks.
- The merged dataset contains AOD information under all sky conditions with little sampling bias.
- The merged dataset is useful for studying long-term aerosol trends, variability, and climate impacts.

ARTICLE INFO

Article history:
Received 2 December 2015
Received in revised form
18 February 2016
Accepted 23 February 2016
Available online 26 February 2016

Keywords:
Visibility
Aerosol optical depth
Chemical transport model
Spatial variability
Temporal variability
China

ABSTRACT

Long-term visibility measurements offer useful information for aerosol and climate change studies. Recently, a new technique to converting visibility measurements to aerosol optical depth (AOD) has been developed on a station-to-station basis (Lin et al., 2014). However, factors such as human observation differences and local meteorological conditions often impair the spatial consistency of the visibility converted AOD dataset. Here we further adopt AOD spatial information from a chemical transport model GEOS-Chem, and merge visibility inferred and modeled early-afternoon AOD over East China on a 0.667° long. × 0.5° lat. grid for 2005–2012. Comparisons with MODIS/Aqua retrieved AOD and subsequent spectral decomposition analyses show that the merged dataset successfully corrects the low bias in the model while preserving its spatial pattern, resulting in very good agreement with MODIS in both magnitude and spatio-temporal variability. The low bias is reduced from 0.10 in GEOS-Chem AOD to 0.04 in the merged data averaged over East China, and the correlation in the seasonal and interannual variability between MODIS and merged AOD is well above 0.75 for most regions. Comparisons between the merged and AERONET data also show an overall small bias and high correlation. The merged dataset reveals four major pollution hot spots in China, including the North China Plain, the Yangtze River Delta, the Pearl River Delta and the Sichuan Basin, consistent with previous works. AOD peaks in spring-summer over the North China Plain and Yangtze River Delta and in spring over the Pearl River Delta, with no distinct seasonal cycle over the Sichuan Basin. The merged AOD has the largest difference from MODIS over the Sichuan Basin. We also discuss possible benefits of visibility based AOD data that correct the sampling bias in MODIS retrievals related to cloud-free sampling and misclassified heavy haze conditions.

1. Introduction

Surface visibility measurements can be used to infer aerosol pollution (Noll et al., 1967; White and Roberts, 1977; Park et al., 2006), and because visibility has been routinely monitored for decades at many locations, they could be potentially useful in studying long-term aerosol trends. Therefore, many attempts have been made to estimate aerosol loadings from visibility data (e.g. Husar et al., 2000; Qian and Giorgi, 2000; Che et al., 2007; Vautard et al., 2009; Qin et al., 2010; Wang et al., 2009, 2012). Most previous studies assumed exponentially decreasing aerosol vertical profiles with a fixed scale height when converting surface measurements to column aerosol optical depth (AOD). More recently, a study by Lin

* Corresponding author.
E-mail address: linjt@pku.edu.cn (J. Lin).

http://dx.doi.org/10.1016/j.atmosenv.2016.02.037
1352-2310/

et al. (2014) took advantage of aerosol vertical distribution simulated by the nested GEOS-Chem chemical transport model (CTM) to yield more realistic AOD estimation. Initial point-by-point comparison with validated MODIS AOD data at individual stations indicated satisfying agreement in both the magnitude and seasonal cycle. Nonetheless, as visibility measurements are only available from scattered stations, the converted AOD lacks sufficient spatial coverage. Moreover, because visibility measurements are subjective to human errors, and that the data may be affected by very local meteorological or pollution conditions, the consistency in spatial variability is relatively low between visibility converted AOD and MODIS. In other words, the visibility dataset alone may not well reflect the spatial variation of aerosols that is necessary for long-term climate forcing studies. This limitation may be overcome by taking advantage of the spatial variability simulated by CTMs.

Driven by emissions and meteorological inputs, CTMs simulate chemical, transport and deposition processes of gaseous and aerosol constituents in the atmosphere. Driven by assimilated meteorological fields, the GEOS-Chem CTM has been shown to capture the major aerosol variability (Bey et al., 2001; van Donkelaar et al., 2013; Zhang et al., 2015). However, modeled AOD may have certain biases due to errors in emissions, chemical mechanisms, and/or meteorological inputs. For example, Heald et al. (2006) showed that on average GEOS-Chem AOD is lower than MODIS by a factor of two over the Pacific and continental US. Our previous study (Lin et al., 2014) and present analysis (see Section 3) also show GEOS-Chem underestimates MODIS AOD over China.

Because visibility converted AOD lacks adequate spatial information while GEOS-Chem AOD suffers from biases, it is rationale to combine the strengths of these two datasets for improved spatial variability and accuracy. For this reason, we used a simple 2-D interpolation method to merge the visibility converted AOD with GEOS-Chem simulated AOD. This new dataset corrects the low bias in GEOS-Chem AOD while preserving its consistent spatial information; it is thus more suitable for climatological studies, especially during periods when no satellite data are available.

In this study, we evaluate the spatial-temporal variability of the merged AOD at 550 nm over East China (101.25°E–126.25°E, 19°N–46°N) from 2005 to 2012. Monthly mean data for the early afternoon (at the MODIS/Aqua overpass time) are derived from daily data and are analyzed here. Section 2 introduces the visibility converted AOD over 2005–2012, the corresponding GEOS-Chem AOD, and the method used to merge the two datasets. A comparison to AERONET data is also given. Section 3 presents the merged dataset and comparison with MODIS/Aqua AOD in terms of spatial and temporal variability. Section 4 briefly discusses the data sampling issues relevant to the merged and MODIS data for aerosol inference. A summary is given in Section 5.

2. Data and methodology

2.1. Visibility converted AOD

We convert the visibility data to AOD at 550 nm at 253 stations over East China from January 2005 through December 2012. The conversion methodology is presented in detail by Lin et al. (2014). Briefly, near surface Aerosol Extinction Coefficient (AEC) is first calculated from a quality-controlled 3-hourly visibility measurement in the absence of precipitation and fogs, then a temporally and spatially coincident AOD to AEC ratio modeled by GEOS-Chem is used to convert near surface AEC to column AOD. In this way, the knowledge of model aerosol profile is involved, instead of assuming a uniform exponential vertical distribution. The resulting AOD product is thus more realistic. Here, we calculate for each day visibility converted AOD in the early afternoon, by linearly interpolating the 3-hourly data to the MODIS/Aqua overpass time. The station-specific visibility converted AOD in 2006 is validated with MODIS data and ground-based AOD measurements by Lin et al. (2014).

2.2. GEOS-Chem AOD

GEOS-Chem simulates the AOD at 550 nm over 2005–2012 with a model spin-up period in 2004. Model results are outputted every day at the MODIS/Aqua overpass time. The model setups are described in detail by Lin et al. (2015). Briefly, we use the nested GEOS-Chem version 9-02 over Asia (Chen et al., 2009) at 0.667° long. × 0.5° lat. with 47 vertical layers and 10 roughly equal-spaced layers below 850 hPa. The model is driven by the GEOS-5 assimilated meteorology, and it is run with the full gaseous chemistry (Mao et al., 2013) and online aerosol calculations. Aerosols simulated include sulfate-nitrate-ammonium particles (Park et al., 2004), black carbon and primary organic carbon (Park et al., 2003; Wang et al., 2011a), natural dusts (Fairlie et al., 2007), and sea salts (Jaeglé et al., 2011). Aerosol optical properties account for the hygroscopic growth; see Drury et al. (2010) for detailed descriptions. Vertical mixing in the boundary layer follows a non-local scheme implemented by Lin and McElroy (2010), and convection adopts the relaxed Arakawa-Schubert scheme (Rienecker et al., 2008).

Anthropogenic emissions of nitrogen oxides (NOx), carbon monoxide, non-methane volatile organic compounds (NMVOCs) and sulfur dioxide are taken from the MEIC inventory (www.meicmodel.org, base year is 2008) over China and from the INTEX-B inventory (Zhang et al., 2009, base year is 2006) for other Asian countries. Anthropogenic emissions of black carbon and primary organic carbon are from INTEX-B. Anthropogenic emissions of ammonia over China are from Huang et al. (2012) (base year is 2008) and from Streets et al. (2003) for other Asian counties (base year is 2000). Chinese anthropogenic NOx emissions are scaled from the base year to other years according to the DOMINO v2 satellite nitrogen dioxide data (Boersma et al., 2011). No inter-annual variations are applied to anthropogenic emissions for other species and/or regions due to lack of information. Biomass burning emissions are taken from the monthly GFED v3 dataset (van der Werf et al., 2010). Biogenic emissions of NMVOCs follow MEGAN v2 (Guenther et al., 2012). Soil emissions of NOx follow Hudman et al. (2011). Lightning emissions of NOx are parameterized based on cloud top heights (Price and Rind, 1992) with a further adjustment according to the OTD/LIS satellite measurements (Murray et al., 2012). Dust particles are emitted with the DEAD scheme (Fairlie et al., 2007), and emissions of sea salts are parameterized by Jaeglé et al. (2011).

2.3. Merging visibility converted AOD and GEOS-Chem AOD

We combine visibility converted and GEOS-Chem simulated AOD to produce a new "merged" AOD dataset on a 0.667° long. × 0.5° lat. grid. For each day, we find for a given grid cell all stations within a 2° radius of the grid cell center (see Fig. 1a for station counts corresponding to each model grid box), calculate the ratios of visibility converted over GEOS-Chem AOD, and then use the median value of the ratios to scale the modeled AOD at the grid cell. We discard extreme cases where the median ratio is above 5 or below 0.2, or where the resulting merged AOD exceeds a value of 5.

The monthly average merged AOD is consistent with the AERONET data (Holben et al., 1998) with a small bias and high correlation. We select all five AERONET sites within the study domain that have at least two years of data, including Beijing, Xianghe,

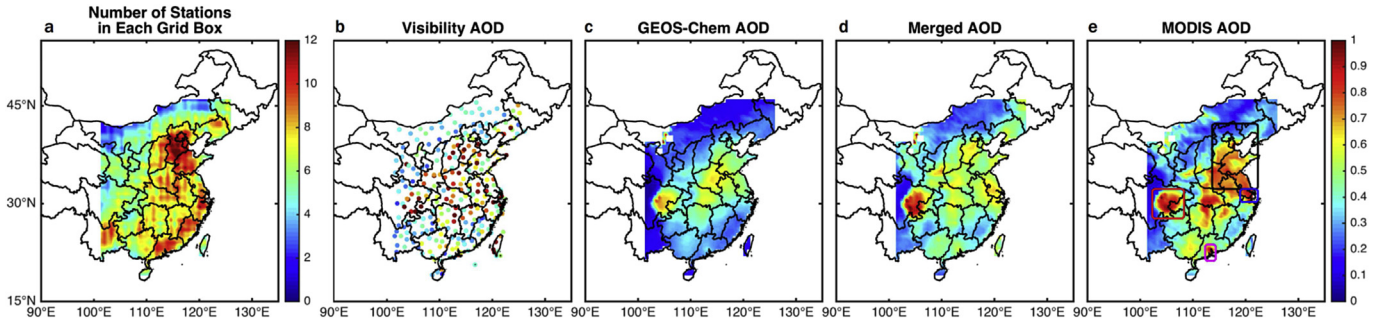

Fig. 1. Number of stations within a 2° radius of each grid cell (a), and multi-year mean visibility converted AOD (b), GEOS-Chem AOD (c), merged AOD (d) and MODIS AOD (e). It is clearly seen that the merged AOD largely correct the low bias in GEOS-Chem AOD. The boxes in (e) mark the key regions for further examination, including the North China Plain (black), the Yangtze River Delta (blue), the Pearl River Delta (magenta), and the Sichuan Basin (red).

Hong Kong PolyU, Taihu, and SACOL (Huang et al., 2008). The geographic information of these sites is depicted in Fig. 2. We collect the level 2 quality-assured AERONET data from the official web page (http://aeronet.gsfc.nasa.gov/), and then derive the AOD data at 550 nm from values at 440 nm using the accompanying Ångstrom exponent data for 440–675 nm (Lin et al., 2014). For comparison, the daily merged AOD data at the grid cell covering a given site are sampled coincidently with valid AERONET data, followed by an averaging process to derive monthly means. Fig. 2 shows that the monthly average merged AOD data reproduce the seasonal and interannual variations of AERONET data for most sites ($R = 0.68–0.81$) but SACOL ($R = 0.35$). At Beijing, Xianghe, Hong Kong PolyU and Taihu, the merged AOD captures the spring-summer highs and wintertime lows of AERONET data fairly well. The merged data underestimate the seasonal AERONET peaks over 2006–2008 at Xianghe; however, these AERONET peaks are not clearly shown in the nearby Beijing site, indicating a potential local influence not expected to be captured by the merged dataset. The low consistency at SACOL, located in a semi-arid region (Huang et al., 2008), is related to the dusty environment with an increased difficulty in converting near-surface visibility to AOD. Overall, the merged AOD biases are only +0.02 at Beijing, −0.06 at Xianghe, −0.01 at Hong Kong PolyU, −0.11 at Taihu, and +0.05 at SACOL. The underestimate at Taihu is contributed mainly by a slight systematic bias over 2005–2008.

Currently there are only a few AERONET sites with multi-year data for our evaluation. Further site-specific evaluation can be done by comparison with Chinese ground-based AOD networks CARSNET (Che et al., 2009) and CSHNET (Xin et al., 2007), when these data become available to allow for a spatio-temporally comprehensive ground-based data base. Our previous study (Lin et al., 2014) have shown very good quality in MODIS/Aqua Collection 5.1 data over East China by comparison with ground-based AERONET, CARSNET and CSHNET data in 2006 (bias = −0.05 or −10%, R = 0.85, across a total of 26 sites). Therefore in the following sections, we will use a gridded MODIS/Aqua AOD dataset to conduct more comprehensive evaluation of the spatio-temporal variability of the merged data.

2.4. MODIS/aqua AOD

Collection 5.1 level 2 AOD product at 550 nm from MODIS/Aqua (Levy et al., 2007, 2010) are used to evaluate the merged AOD product. Our previous analysis (Lin et al., 2014) showed that the MODIS/Aqua data are consistent with ground-based AERONET, CARSNET and CSHNET networks over East China in 2006, with a low bias (−0.05 or −10%) and a high correlation coefficient (0.85) across a total of 26 sites, consistent with the findings of other works (Wang et al., 2010, 2013b). For each day, we map the nominal 10 km × 10 km level 2 pixels to the 0.667° long. × 0.5° lat. grid to match GEOS-Chem and merged AOD.

3. Spatio-temporal variability of gridded merged AOD

This section analyzes the spatial and temporal variability of aerosol loadings over East China using the gridded merged dataset, complemented by a comparison with MODIS. We further use Combined Principal Component Analysis (CPCA, Li et al., 2014) to examine the spatio-temporal coherency with MODIS data.

We compare the merged AOD to the MODIS data on a monthly mean basis. We average the daily data to derive monthly means. The merged AOD is available for about 86% of the days on average (except when the visibility data are missing or discarded at the data processing step), while MODIS data are only for cloud-free situations. To correct for the sampling difference in comparing with MODIS, we calculate the difference for each day between modeled AOD coincident with the merged data and with MODIS data, and then use the monthly average of these daily differences to adjust the monthly mean merged AOD. A similar procedure is done for visibility converted AOD data. All data presented in this section are based on the MODIS sampling. In Section 4, we will further discuss the sampling bias relevant to the spatio-temporal analysis.

3.1. Annual mean, seasonal variation and time series

Fig. 1 shows the multi-year average of the station-specific visibility converted AOD (Fig. 1b) over East China. While the visibility AOD data display a rough spatial pattern, e.g., higher over the eastern regions and lower over the west and northwest, there are clear inconsistencies in the AOD magnitude between nearby stations, which may result from the errors discussed in the Introduction Section. The merged AOD data (Fig. 1d) remove most of these inconsistencies, by combining the spatial information of the modeled AOD (Fig. 1c).

Fig. 1c–e shows the multi-year average annual mean AOD distribution over East China from GEOS-Chem (Fig. 1c), the merged dataset (Fig. 1d) and MODIS (Fig. 1e). Overall, there are several hot spots indicated in all three datasets, namely the North China Plain (black box in Fig. 1e), the Yangtze River Delta (blue box), the Sichuan Basin (red box) and the Pearl River Delta (magenta box). Annual mean AOD could reach 1 over these areas, a sign of significant pollution. There is an obvious low bias in GEOS-Chem AOD (Fig. 1c), which is largely corrected by merging with visibility data (Fig. 1d). To examine the correction more quantitatively, Table 1 lists the multi-year bias and Root Mean Square Error (RMSE) of

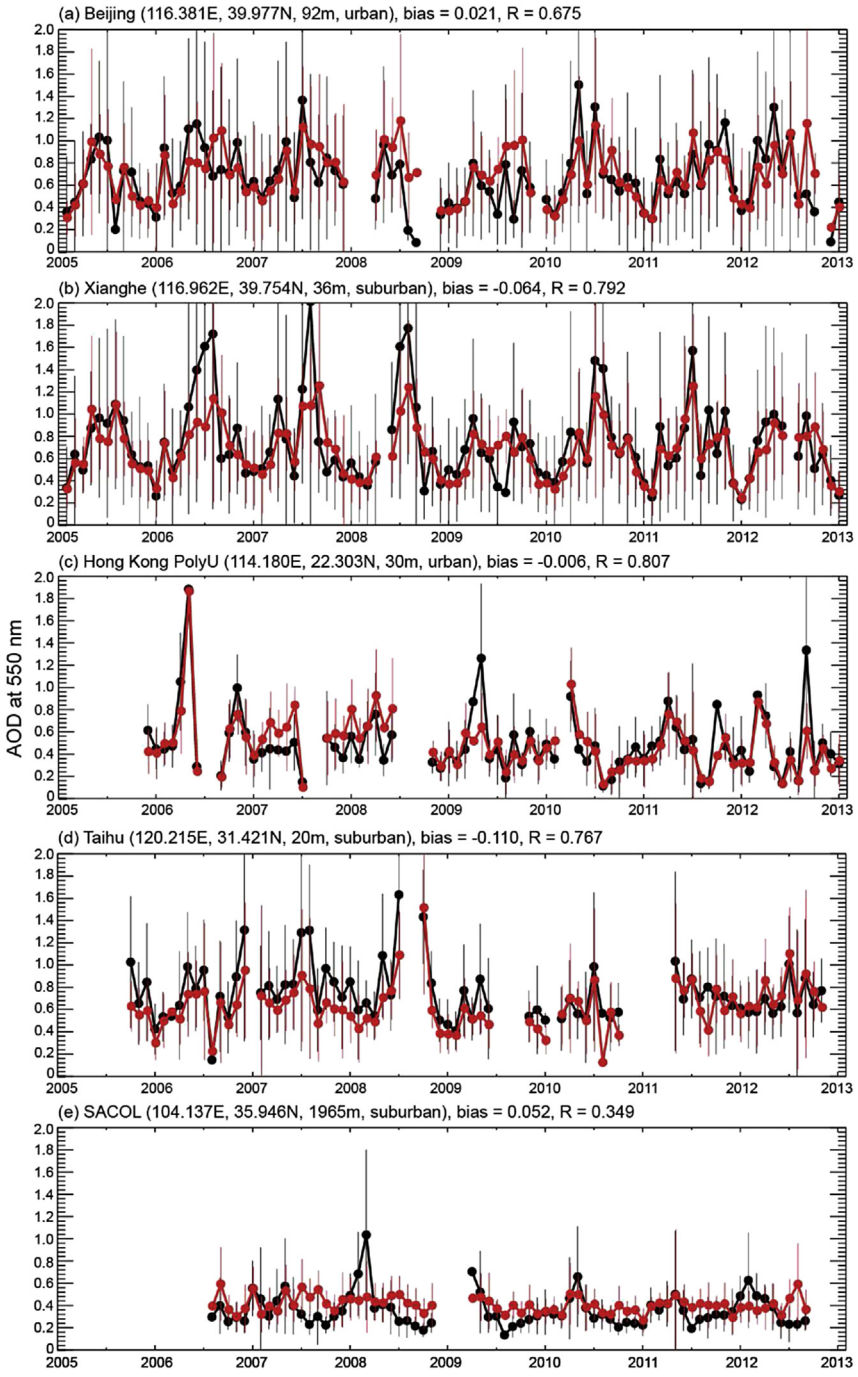

Fig. 2. Time series of the monthly average merged AOD (red) and AERONET data (black). The merged AOD are sampled from days with valid AERONET data. The vertical bars indicate the standard deviations in any given month. The geographic information (longitude, latitude, altitude) of each site and the bias and correlation for the merged AOD relative to AERONET are also given. (For interpretation of the references to color in this figure legend, the reader is referred to the web version of this article).

Table 1
Bias and RMSE between GEOS-Chem and MODIS, and between merged data and MODIS for the five regions.

Bias/RMSE	East China	North China Plain	Yangtze River Delta	Pearl River Delta	Sichuan Basin
GEOS-Chem vs. MODIS	−0.10/0.12	−0.15/0.18	−0.19/0.22	−0.20/0.24	−0.12/0.19
Merged vs. MODIS	−0.04/0.11	−0.05/0.15	−0.14/0.15	−0.11/0.14	0.02/0.24

GEOS-Chem and merged AOD relative to MODIS. The bias correction ranges from 0.05 (or 26%) for the Yangtze River Delta to 0.10 (or 67%) for the North China Plain. Averaged over East China, the low bias is reduced from 0.10 to 0.04, a 60% correction.

The remaining low bias in the merged dataset, which is particularly significant over the North China Plain (Fig. 1d, e), may be

because GEOS-Chem underestimates the AOD to AEC ratio by concentrating aerosols near the ground too much (Ford and Heald, 2012; van Donkelaar et al., 2013). Based on a comparison with the multi-year average CALIOP aerosol profiles, van Donkelaar et al. (2013) showed that GEOS-Chem simulated summertime climatological aerosol profiles underestimate the columnar to near-surface aerosol ratio by up to 30% over the North China Plain. It is conceivable to use the multi-year average CALIOP aerosol profiles to adjust the climatological model profiles, with one complication that the low spatio-temporal coverage of CALIOP (16 days for one global mapping) leads to enhanced noises (van Donkelaar et al., 2013) and also prevents a month-by-month adjustment necessary for our merged dataset. On the other hand, our previous analysis for 2006 (Lin et al., 2014) showed that MODIS/Aqua slightly underestimates ground-based AOD retrievals from AERONET, CARSNET and CSHNET (bias = −0.05 or −10%) with a high correlation (R = 0.85) based on a point-to-point comparison across a total of 26 sites. This suggests that the uncertainties in MODIS data are unlikely the main reason for the overall underestimate (relative to MODIS) in the merged AOD dataset.

Aerosols over the study domain also exhibit distinct seasonal variability, as shown in Fig. 3. Based on MODIS data, the AOD over the North China Plain is higher in spring (MAM) and summer (JJA) but lower in fall (SON) and winter (DJF). Similar patterns are found for the Yangtze River Delta and Pearl River Delta. For the Sichuan Basin, AOD peaks during the winter and spring seasons. These general features were also found by previous satellite-based studies (e.g., Li et al., 2003; Su et al., 2010; Luo et al., 2014). GEOS-Chem roughly captures these seasonal variations, albeit with an overall low bias. However, the spring time high AOD over most eastern and southern regions and the Sichuan Basin is not well represented. After merging with visibility AOD, the low bias is again effectively reduced, especially over the east and the south. The merged data show consistent seasonal variations with MODIS AOD over most regions. For the Sichuan Basin, the fall season AOD is also increased to a magnitude comparable with the spring time data, somehow shifting the seasonal cycle there. This may be due to the year-round high relative humidity and complex terrains there and will be further illustrated below.

To examine the seasonal cycle for different regions and to compare with MODIS in more detail, Fig. 4 shows the mean seasonal cycle over the four hot spot regions (North China Plain, Yangtze River Delta, Pearl River Delta and Sichuan Basin) and the entire East China. The "r" values in the figure indicate the correlation between the GEOS-Chem/merged AOD seasonal cycle with that of MODIS. Fig. 4 shows that by combining with visibility AOD, not only has the low bias been corrected in GEOS-Chem, but the correlation with MODIS has also become much higher for most regions. Both the merged and MODIS data show that over the North China Plain and Yangtze River Delta, AOD peaks in spring-summer, especially in June, while it reaches the lowest values in the winter months, consistent with previous ground-based AOD analyses (Yu et al., 2009; Wang et al., 2011b; Xia et al., 2013; Lin et al., 2014). Over the Pearl River Delta, AOD is the highest in spring, especially in March.

Fig. 4 shows no distinct seasonal cycle of AOD over the Sichuan Basin. The correlation between the merged AOD and MODIS is low, likely due to the seasonally invariant high relative humidity condition there (Chen and Xie, 2013; Wang et al., 2013a), which complicates the conversion from visibility to AOD as it requires an accurate model representation of vertically-resolved aerosol hygroscopic growth. The complex terrain there may also have reduced the spatial representativeness of visibility measurements (Wang et al., 2013a). These complications have also resulted in a low correlation (0.3) between GEOS-Chem and MODIS AOD.

Finally, Fig. 5 compares the time series of the three monthly datasets for the study period. This comparison better demonstrates the effect of combing visibility and modeled AOD fields, by improving the magnitude, seasonality and interannual variability. For all East China, the merged AOD closely agrees with MODIS in both magnitude and variability. Compared with GEOS-Chem AOD, the merged data not only correct the bias but also reduce the phase differences, resulting in a 0.9 correlation. The agreement is also significantly improved for the North China Plain, Yangtze River Delta and Pearl River Delta, with correlations well above 0.75. For the Sichuan Basin, the AOD magnitude agrees better, although there are still some mismatches in temporal variability. Over the North China Plain and Yangtze River Delta, both MODIS and merged data show growing AOD during 2005–2008 along with Chinese economic growth (Lin et al., 2010), followed by a sharp decline in 2009 due to the economic downturn (Lin and McElroy, 2011) and sulfur emission controls (Lu et al., 2011). The trends are broadly consistent with previous aerosol trend studies (Boys et al., 2014; Lin et al., 2013; Cheng et al., 2013; Gong et al., 2014).

In sum, the visibility-GEOS Chem merged AOD dataset combines the strengths of both components, corrects the low bias in GEOS-Chem by 60% averaged over East China, and meanwhile well represents the spatial and temporal variability of aerosols over East China. Next we will use a spectral analysis to further examine the dominant modes of variability.

3.2. CPCA analysis

CPCA is a spectral technique to decomposing multiple multi-dimensional datasets into several major modes of variability. These modes represent the common variability in these datasets, thus can be used on different measurements of the same parameter to evaluate the consistency and discrepancy across the datasets. Li et al. (2014) first introduced CPCA into AOD data inter-comparison and proved the usefulness of this technique. Here we apply the same analysis for cross-comparison between GEOS-Chem, merged and MODIS AOD fields. Detailed mathematical description of the method can be found in Li et al. (2014). Briefly, multiple datasets with the same time span are first combined into one large data matrix, then PCA is performed on the combined matrix to extract the time series (PCs), and the PCs are finally projected back onto each individual dataset to obtain the spatial pattern (EOFs). In this way, each dataset has a spatial pattern while sharing a common time series, thus comparison can be quantitatively performed on the spatial patterns alone. An important note is that by combing different datasets, we are assuming equal weights. This assumption is suitable for the multiple AOD fields used here; however, caution must be taken when combing datasets of different parameters.

CPCA is first performed on the full dataset combining MODIS AOD, GEOS-Chem AOD and the merged AOD. It produces 96 modes corresponding to 96 months in total, and Fig. 6 shows the variances explained by the first 20 modes. Based on the sharp drop in variance from Mode 3 to Mode 4 and the small fractions of variance explained by modes 4 and onwards, we retain the first three modes for further analyses. Their spatial patterns and time series are displayed in Fig. 7. For the first two modes, the PCs both exhibit distinct seasonal cycles, while the spatial patterns highlight northern and southern East China, respectively, thus they represent the seasonal variability over these two regions. PC 1 indicates that AOD over northern East China (mostly the North China Plain) peaks during the late spring to early summer, consistent with previous results. The seasonal cycle for southern East China is less evident, but is in general highest in spring and lowest in fall. Mode 3 captures a weak variability around the Yangtze River Delta region, which has a rough semi-annual seasonal cycle with dual peaks in

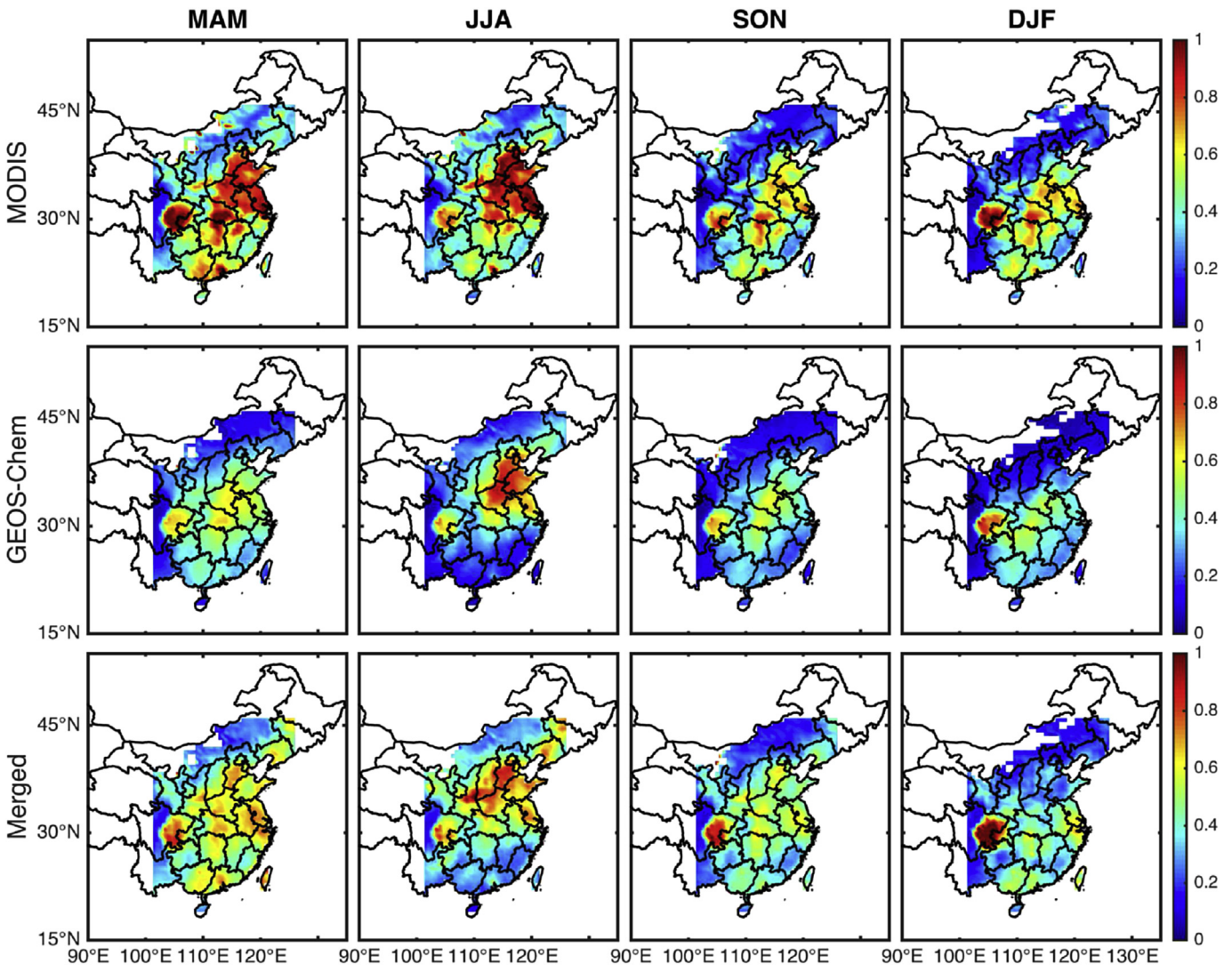

Fig. 3. MODIS (top row), GEOS-Chem (middle row) and the merged (bottom row) AOD averaged for the four seasons: spring (MAM), summer (JJA), fall (SON) and winter (DJF).

spring and winter. This mode could be a modulation of the seasonal variability. Qualitatively, both GEOS-Chem and merged AOD agree with MODIS in terms of spatial distribution. However, the merged dataset still shows certain quantitative improvements compared with GEOS-Chem. For example, in Mode 2, GEOS-Chem has a low bias in southern East China, while in Mode 3, it has a slight high bias in the central-southern East China extending from Anhui to Chongqing. The merged dataset is more coherent with MODIS over these regions.

We continue to examine the interannual variability by performing CPCA on the de-seasonalized (removal of multi-year averaged seasonal cycle) dataset. Again based on the change of variance explained curve (Fig. 6), we consider the first three modes as dominant. Fig. 8 shows the first three modes representing the interannual variability for all East China, northern East China (mostly the North China Plain) and the Yangtze River Delta, respectively. Similar to the above results, there is high overall agreement across the three datasets. The insufficient variability in GEOS-Chem Mode 1 has been greatly improved by the merged dataset. PCs 1 and 3 reveal a positive trend until 2008, broadly consistent with the aerosol trends over East China found by Boys et al. (2014), Cheng et al. (2013) and Gong et al. (2014).

4. Discussions on sampling bias

It is well known that passive sensors such as MODIS can only retrieve aerosol information in cloud free areas, as the high reflectivity by clouds conceals any signal from aerosols. However, visibility measurements are available under all sky conditions, therefore in theory it contains more complete information than MODIS. To investigate how large a bias cloud-free sampling would introduce to MODIS AOD, we compare GEOS-Chem AOD with and without sampling with MODIS data. Fig. 9a–c shows that the sampling with MODIS clearly results in an overall low bias in AOD estimate, which could reach as high as 0.2 for many areas. The MODIS sampling also leads to a similar bias in the merged AOD data (Fig. 9d, e). The merged AOD (without MODIS sampling) is much less susceptible to a sampling bias since data are available for ~86% of days.

Another problem with MODIS, particularly over East China, is that it tends to miss heavy pollution scenes. This is likely because the reflectivity by aerosols is comparable to that of clouds under these heavily polluted conditions and the retrieval algorithm screened out these data as clouds. Fig. 10 shows an example on January 9th, 2015, when there was a heavily polluted air mass

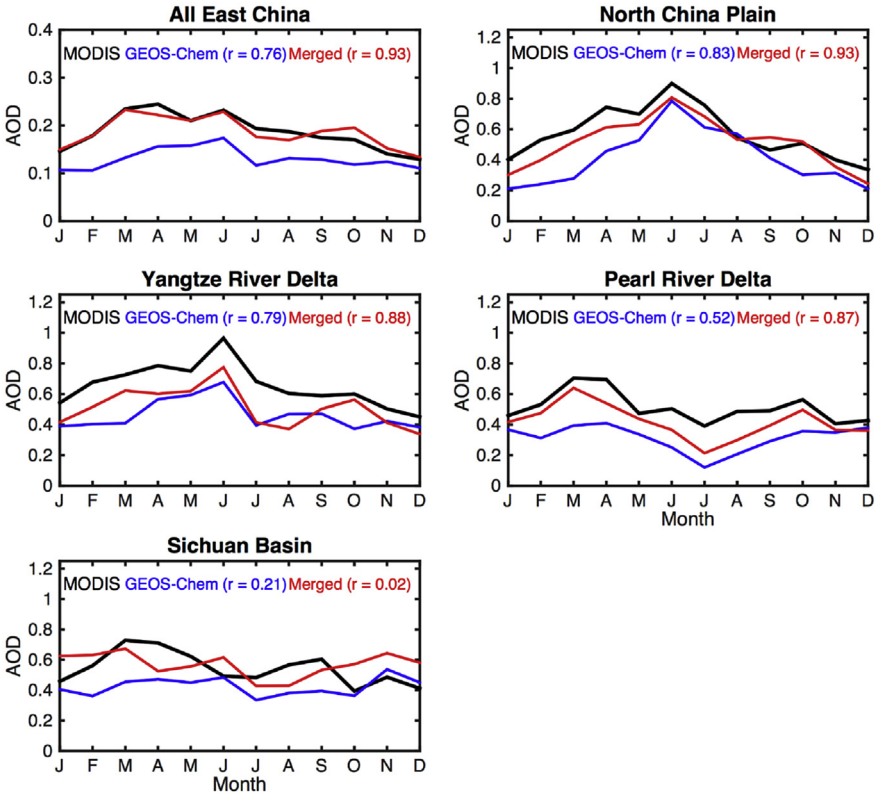

Fig. 4. Multi-year mean seasonal variability of AOD for the five representative regions. The r values in the parentheses denote the correlation between the corresponding time series and MODIS. See Fig. 1e for region definitions.

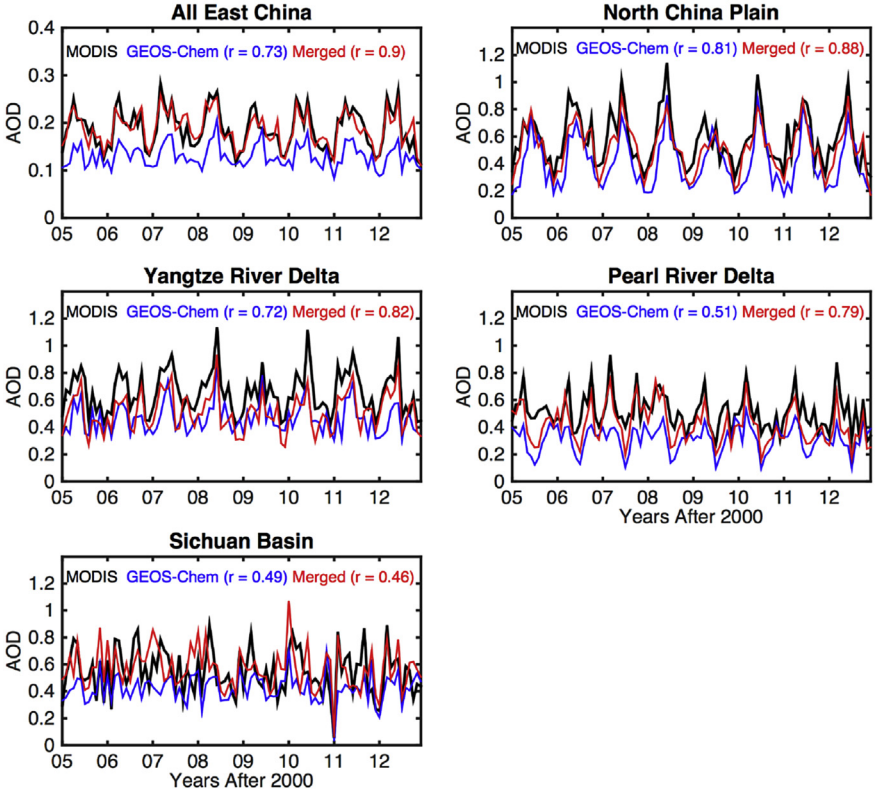

Fig. 5. Monthly time series of the three AOD datasets for the five regions. The r values in the parentheses denote the correlation between the corresponding time series and MODIS. See Fig. 1e for region definitions.

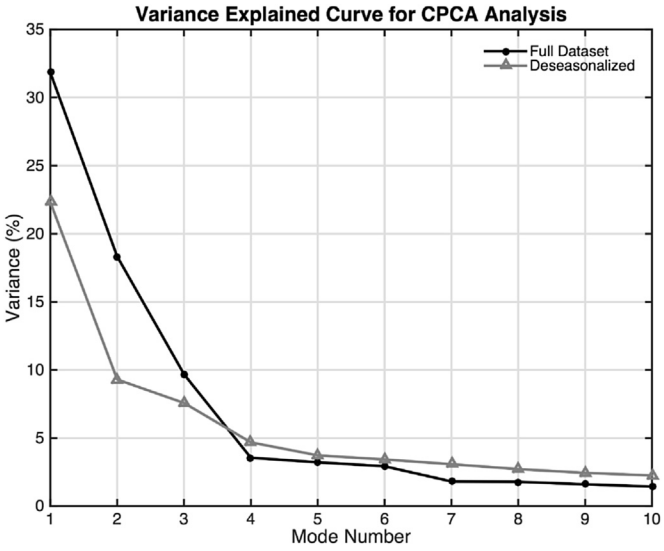

Fig. 6. The variances explained by the first 20 modes of CPCA analysis of MODIS, GEOS-Chem and the merged AOD datasets, without (black line) and with (grey line) removing the seasonal cycle.

covering East China extending from the Shandong Peninsula to the Yangtze River Delta (red box in the true color image). However, there is no AOD retrieval over this region in the level 2 MODIS AOD product for the same scene (right panel). Another representative example concerns the extreme pollution in January 2013 during which month northern East China experienced very severe and long-lasting pollution (Che et al., 2014; Sun et al., 2014). Here we extend to January 2013 the GEOS-Chem simulation and aerosol data processing. Fig. 11 shows the monthly mean MODIS AOD and visibility-GEOS Chem merged AOD for this month. We can see that there is no MODIS retrieval for northern East China, especially the most polluted regions of Hebei and Shandong Provinces, while the merged dataset has more complete spatial information and reveals the heavy pollution.

Currently there are no simple observation-based methods to accurately quantify the quality of visibility-inferred AOD data under cloudy or heavy pollution conditions. Qualitatively, one could use ground-based particulate matter (PM) mass concentration measurements (that are done under all sky conditions) to differentiate various cloud and pollution situations for assessing visibility-inferred AOD data. However, such assessment is complicated by the different dependence of PM mass concentration, visibility and AOD on meteorological conditions such as boundary layer mixing and water vapor content. Nonetheless, as MODIS data are limited by cloud-free sampling and misclassified heavy pollution, visibility converted AOD, especially when combined with model simulations, offers potentially more complete aerosol information with reasonable quality.

5. Summary

Visibility measurements could provide long-term aerosol information, thus are potentially valuable for climate studies. For more complete coverage and better representation of spatial variability, we take advantage of a GEOS-Chem aerosol simulation and develop a technique to merge visibility converted AOD with GEOS-Chem AOD. Monthly mean data for the early afternoon (at the MODIS/Aqua overpass time) are produced and analyzed. Comparisons with MODIS/Aqua AOD indicate that the merged dataset largely corrects the bias in modeled AOD field. The agreement in

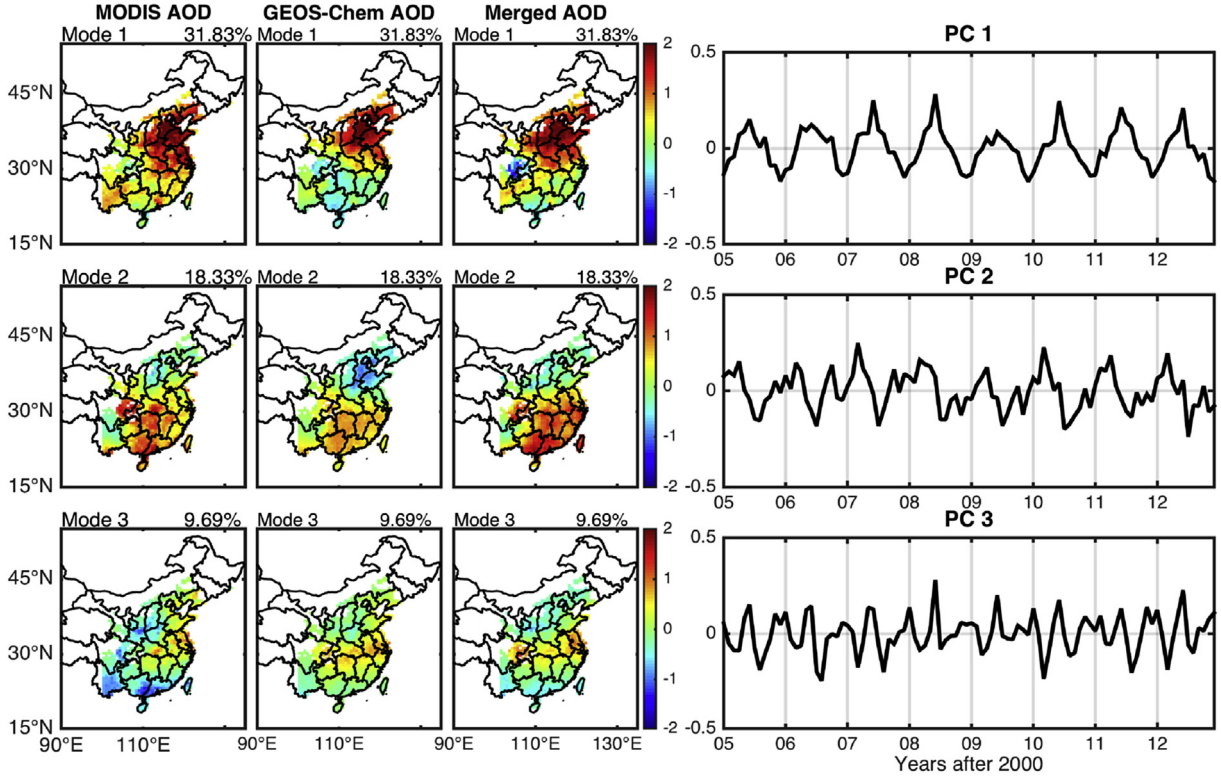

Fig. 7. The first three CPCA modes, with seasonality included. The first two modes represent seasonal variability for northern and southern East China, respectively. The third mode shows a semi-annual cycle of the Yangtze River Delta region. The three datasets qualitatively agree while the merged data agrees better with MODIS, especially for Modes 1 and 2.

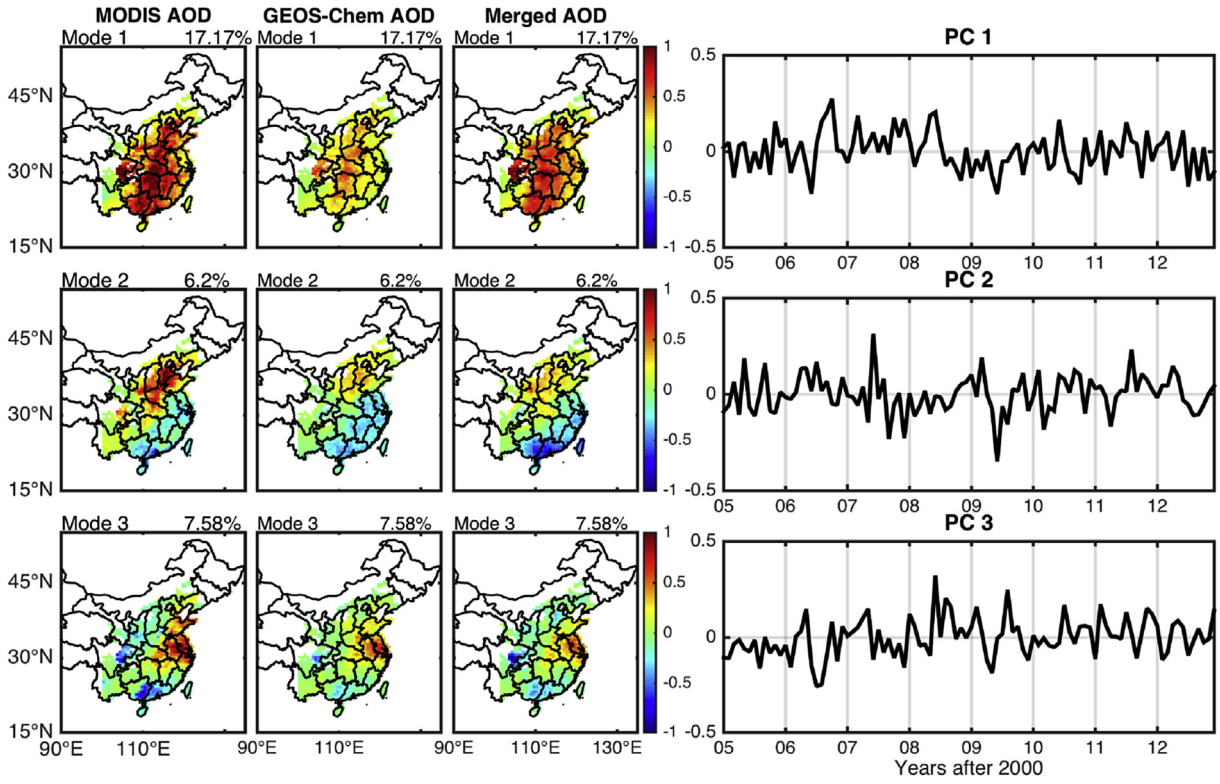

Fig. 8. The first three de-seasonalized CPCA modes, representing interannual variability. The merged dataset still agrees well with MODIS.

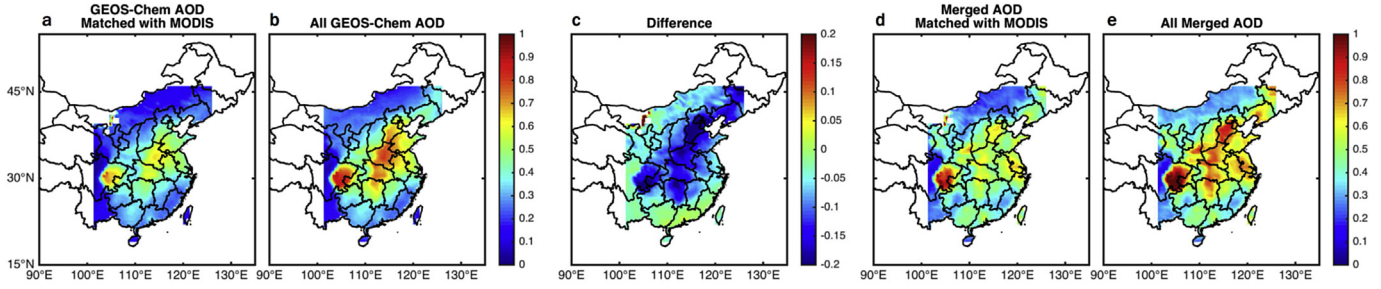

Fig. 9. Possible MODIS bias due to its cloud-free only sampling. Panel a shows GEOS-Chem AOD matched with MODIS observations, panel b is all GEOS-Chem AOD, and panel c is their difference. Panels d and e show the merged AOD with and without correction for MODIS sampling, respectively. We can see that there is a low bias by as much as −0.2 due to the MODIS sampling.

spatial and temporal variability is also improved, especially over the North China Plain and the south. Comparisons with AERONET AOD data also show overall good consistency with a small bias and high correlation.

Using the new merged dataset, we identify four major AOD hot spots in East China, namely the North China Plain, the Yangtze River Delta, the Pearl River Delta and the Sichuan Basin. Most regions exhibit distinct seasonal variability. For the North China Plain, AOD is the highest from late spring to early summer and the lowest in winter. While for southern East China (including the Pearl River Delta), AOD usually peaks in the early spring season. These spatial and seasonal patterns are consistent with many previous studies (e.g., Li et al., 2003; Yu et al., 2009; Su et al., 2010; Wang et al., 2011b; Xia et al., 2013; Lin et al., 2014; Luo et al., 2014). Interannually, the merged AOD over the North China Plain and Yangtze River Delta show a growth until 2008 followed by a sharp decline in 2009, also consistent with previous findings (Boys et al., 2014; Cheng et al., 2013; Gong et al., 2014). These results indicate a correct representation of AOD variability by the merged dataset.

The current study focuses on the recent decade when MODIS data are available for comparison, as the major goal is to present the new merged dataset and to evaluate its spatio-temporal variability. The primary advantage of this dataset, however, is its usefulness in studying long-term aerosol changes. Visibility measurements started well before the satellite era, and GEOS-Chem simulations with assimilated meteorological fields are also possible since 1979. Therefore, we will next process the data all through 1979, expand the study domain to worldwide locations, and use the data to examine the long-term aerosol trends. This research will provide important insights into the role of aerosols in the global and regional climate changes. Our data will be available for public use at http://www.atmos.pku.edu.cn/acm/acmProduct.html.

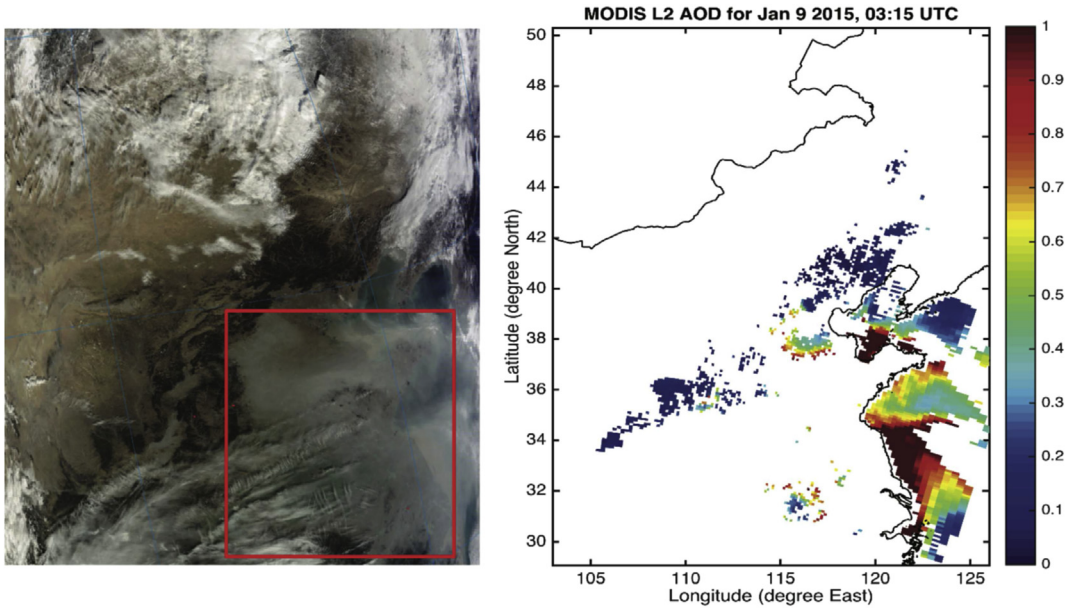

Fig. 10. MODIS true color image (left) and Level 2 AOD retrieval (right) for January 9th, 2015 over the North China Plain. The true color image shows heavy pollution spreading from the Shandong Peninsula to the Yangtze River Delta (marked by red box). However, there is no AOD retrieval over land for this region.

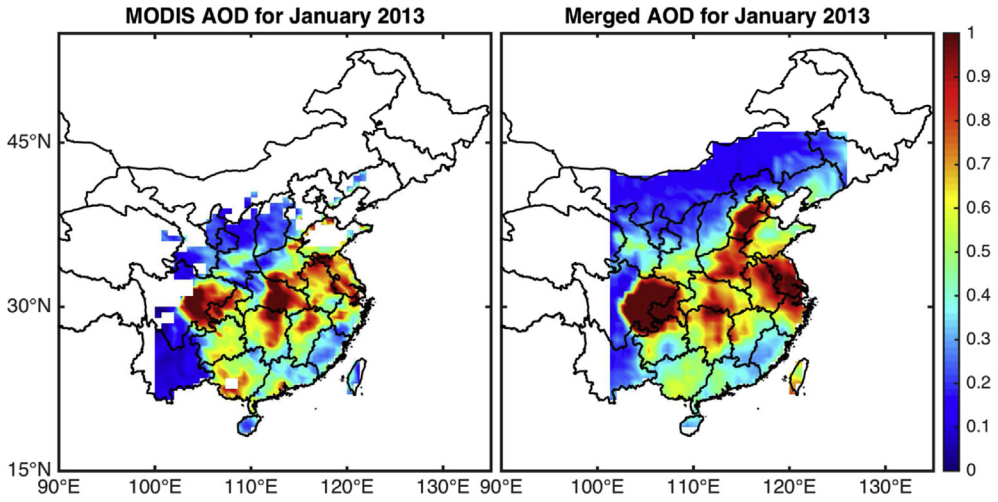

Fig. 11. Monthly average MODIS AOD (left) and merged AOD (without correction for MODIS sampling, right) for January 2013. During this month, northern East China is known to have experienced heavy pollution but MODIS does not have AOD retrievals, while merged dataset has more complete spatial information and shows the heavy pollution.

Acknowledgments

This research is supported by the National Natural Science Foundation of China, grant 41175127 and 41422502, and by the 973 program, grant 2014CB441303. Jing Li is supported by National Natural Science Foundation of China grant 41575018.We acknowledge the free use of MODIS data from NASA and visibility data from NOAA NCDC. We thank the principle investigators (Beijing: Hong-Bin Chen and Philippe Goloub, Xianghe: Pucai Wang and Xiangao Xia, Hong Kong PolyU: Janet Elizabeth Nichol, Taihu: Ronghua Ma, and SACOL: Jianping Huang and Wu Zhang) and their staff for establishing and maintaining the individual AERONET sites.

References

Bey, I., Jacob, D.J., Yantosca, R.M., Logan, J.A., Field, B.D., Fiore, A.M., Li, Q., Liu, H.Y., Mickley, L.J., Schultz, M.G., 2001. Global modeling of tropospheric chemistry with assimilated meteorology: model description and evaluation. J. Geophys. Res. 106, 23073.

Boersma, K.F., Eskes, H.J., Dirksen, R.J., A, R.J.v.d, Veefkind, J.P., Stammes, P., Huijnen, V., Kleipool, Q.L., Sneep, M., Claas, J., Leitão, J., Richter, A., Zhou, Y., Brunner, D., 2011. An improved tropospheric NO2 column retrieval algorithm for the ozone monitoring instrument. Atmos. Meas. Tech. 4, 1905–1928.

Boys, B., Martin, R., van Donkelaar, A., MacDonell, R., Hsu, N., Cooper, M., Yantosca, R., Lu, Z., Streets, D.G., Zhang, Q., 2014. Fifteen-year global time series of satellite-derived fine particulate matter. Environ. Sci. Technol. 48, 11109–11118.

Che, H., Zhang, X., Li, Y., Zhou, Z., Qu, J.J., 2007. Horizontal visibility trends in China 1981–2005. Geophys. Res. Lett. 34, L24706.

Che, H.Z., Zhang, X.Y., Chen, H.B., Damiri, B., Goloub, P., Li, Z.Q., Zhang, X.C., Wei, Y., Zhou, H.G., Dong, F., Li, D.P., Zhou, T.M., 2009. Instrument calibration and aerosol optical depth validation of the China Aerosol Remote Sensing Network. J. Geophys. Res. Atmos. 114, D03206.

Che, H., Xia, X., Zhu, J., Li, Z., Dubovik, O., Holben, B., Goloub, P., Chen, H., Estelles, V., Cuevas-Agulló, E., Blarel, L., Wang, H., Zhao, H., Zhang, X., Wang, Y., Sun, J., Tao, R., Zhang, X., Shi, G., 2014. Column aerosol optical properties and aerosol

radiative forcing during a serious haze-fog month over North China Plain in 2013 based on ground-based sunphotometer measurements. Atmos. Chem. Phys. 14, 2125–2138.
Chen, Y., Xie, S.-d, 2013. Long-term trends and characteristics of visibility in two megacities in southwest China: Chengdu and Chongqing. J. Air Waste Manag. Assoc. 63, 1058–1069.
Chen, D., Wang, Y., McElroy, M.B., He, K., Yantosca, R.M., Le Sager, P., 2009. Regional CO pollution and export in China simulated by the high-resolution nested-grid GEOS-Chem model. Atmos. Chem. Phys. 9, 3825–3839.
Cheng, Z., Wang, S., Jiang, J., Fu, Q., Chen, C., Xu, B., Yu, J., Fu, X., Hao, J., 2013. Long-term trend of haze pollution and impact of particulate matter in the Yangtze River Delta, China. Environ. Pollut. 182, 101–110.
Drury, E., Jacob, D.J., Spurr, R.J.D., Wang, J., Shinozuka, Y., Anderson, B.E., Clarke, A.D., Dibb, J., McNaughton, C., Weber, R., 2010. Synthesis of satellite (MODIS), aircraft (ICARTT), and surface (IMPROVE, EPA-AQS, AERONET) aerosol observations over eastern North America to improve MODIS aerosol retrievals and constrain surface aerosol concentrations and sources. J. Geophys. Res. Atmos. 115, D14204.
Fairlie, T.D., Jacob, D.J., Park, R.J., 2007. The impact of transpacific transport of mineral dust in the United States. Atmos. Environ. 41, 1251–1266.
Ford, B., Heald, C.L., 2012. An A-train and model perspective on the vertical distribution of aerosols and CO in the Northern Hemisphere. J. Geophys. Res. Atmos. 117, D06211.
Gong, C., Xin, J., Wang, S., Wang, Y., Wang, P., Wang, L., Li, P., 2014. The aerosol direct radiative forcing over the Beijing metropolitan area from 2004 to 2011. J. Aerosol Sci. 69, 62–70.
Guenther, A., Jiang, X., Heald, C., Sakulyanontvittaya, T., Duhl, T., Emmons, L., Wang, X., 2012. The Model of Emissions of Gases and Aerosols from Nature Version 2.1 (MEGAN2. 1): an Extended and Updated Framework for Modeling Biogenic Emissions, vol. 5, pp. 1471–1492.
Heald, C.L., Jacob, D.J., Park, R.J., Alexander, B., Fairlie, T.D., Yantosca, R.M., Chu, D.A., 2006. Transpacific transport of Asian anthropogenic aerosols and its impact on surface air quality in the United States. J. Geophys. Res. Atmos. 111, 3085–3098.
Holben, B.N., Eck, T.F., Slutsker, I., Tanre, D., Buis, J.P., Setzer, A., Vermote, E., Reagan, J.A., Kaufman, Y.J., Nakajima, T., Lavenu, F., Jankowiak, I., Smirnov, A., 1998. AERONET — a federated instrument network and data archive for aerosol characterization. Remote Sens. Environ. 66, 1–16.
Huang, J., Zhang, W., Zuo, J., Bi, J., Shi, J., Wang, X., Chang, Z., Huang, Z., Yang, S., Zhang, B., 2008. An overview of the semi-arid climate and environment research observatory over the Loess Plateau. Adv. Atmos. Sci. 25, 906–921.
Huang, X., Song, Y., Li, M., Li, J., Huo, Q., Cai, X., Zhu, T., Hu, M., Zhang, H., 2012. A high-resolution ammonia emission inventory in China. Glob. Biogeochem. Cycles 26, Gb1030.
Hudman, R.C., Moore, N., Mebust, A.K., Martin, R., Russell, A.R., Valin, L.C., Cohen, R.C., 2011. Steps towards a mechanistic model of global soil nitric oxide emissions: implementation and space based-constraints. Atmos. Chem. Phys. 12, 7779–7795.
Husar, R.B., Husar, J.D., Martin, L., 2000. Distribution of continental surface aerosol extinction based on visual range data. Atmos. Environ. 34, 5067–5078.
Jaeglé, L., Quinn, P.K., Bates, T.S., Alexander, B., Lin, J.T., 2011. Global distribution of sea salt aerosols: new constraints from in situ and remote sensing observations. Atmos. Chem. Phys. 11, 3137–3157.
Levy, R.C., Remer, L.A., Kleidman, R.G., Mattoo, S., Ichoku, C., Kahn, R., Eck, T., 2010. Global evaluation of the Collection 5 MODIS dark-target aerosol products over land. Atmos. Chem. Phys. 10, 10399–10420.
Levy, R.C., Remer, L.A., Mattoo, S., Vermote, E.F., Kaufman, Y.J., 2007. Second-generation operational algorithm: retrieval of aerosol properties over land from inversion of moderate resolution imaging spectroradiometer spectral reflectance. J. Geophys. Res. Atmos. (1984–2012) 112, D13211.
Li, C., Mao, J., Lau, K.-H.A., Chen, J.-C., Yuan, Z., Liu, X., Zhu, A., Liu, G., 2003. Characteristics of distribution and seasonal variation of aerosol optical depth in eastern China with MODIS products. Chin. Sci. Bull. 48, 2488–2495.
Li, J., Carlson, B.E., Lacis, A.A., 2014. Application of spectral analysis techniques in the inter-comparison of aerosol data part III: using combined PCA to compare spatio-temporal variability of MODIS, MISR and OMI aerosol optical depth. J. Geophys. Res. 119, 4017–4042.
Lin, J.-T., McElroy, M.B., 2010. Impacts of boundary layer mixing on pollutant vertical profiles in the lower troposphere: implications to satellite remote sensing. Atmos. Environ. 44, 1726–1739.
Lin, J.-T., McElroy, M.B., 2011. Detection from space of a reduction in anthropogenic emissions of nitrogen oxides during the Chinese economic downturn. Atmos. Chem. Phys. 11, 8171–8188.
Lin, J.-T., Nielsen, C.P., Zhao, Y., Lei, Y., Liu, Y., McElroy, M.B., 2010. Recent changes in particulate air pollution over China observed from space and the ground: effectiveness of emission control. Environ. Sci. Technol. 44, 7771–7776.
Lin, J.-T., Pan, D., Zhang, R., 2013. Trend and interannual variability of Chinese air pollution since 2000 in association with socioeconomic development: a brief overview. Atmos. Ocean. Sci. Lett. 6, 84–89.
Lin, J.-T., van Donkelaar, A., Xin, J., Che, H., Wang, Y., 2014. Clear-sky aerosol optical depth over East China estimated from visibility measurements and chemical transport modeling. Atmos. Environ. 95, 257–267.
Lin, J.-T., Liu, M.Y., Xin, J.Y., Boersma, K.F., Spurr, R., Martin, R., Zhang, Q., 2015. Influence of aerosols and surface reflectance on satellite NO2 retrieval: seasonal and spatial characteristics and implications for NOx emission constraints. Atmos. Chem. Phys. 15, 11217–11241.
Lu, Z., Zhang, Q., Streets, D.G., 2011. Sulfur dioxide and primary carbonaceous aerosol emissions in China and India, 1996–2010. Atmos. Chem. Phys. 11, 9839–9864.
Luo, Y., Zheng, X., Zhao, T., Chen, J., 2014. A climatology of aerosol optical depth over China from recent 10 years of MODIS remote sensing data. Int. J. Climatol. 34, 863–870.
Mao, J., Paulot, F., Jacob, D.J., Cohen, R.C., Crounse, J.D., Wennberg, P.O., Keller, C.A., Hudman, R.C., Barkley, M.P., Horowitz, L.W., 2013. Ozone and organic nitrates over the eastern United States: sensitivity to isoprene chemistry. J. Geophys. Res. Atmos. 118, 11,256–211,268.
Murray, L.T., Jacob, D.J., Logan, J.A., Hudman, R.C., Koshak, W.J., 2012. Optimized regional and interannual variability of lightning in a global chemical transport model constrained by LIS/OTD satellite data. J. Geophys. Res. Atmos. (1984–2012) 117, D20307.
Noll, K.E., Mueller, P.K., Imada, M., 1967. Visibility and aerosol concentration in urban air. Atmos. Environ. 2, 465–475.
Park, R.J., Jacob, D.J., Chin, M., Martin, R.V., 2003. Sources of carbonaceous aerosols over the United States and implications for natural visibility. J. Geophys. Res. Atmos. 108, 4355.
Park, R.J., Jacob, D.J., Field, B.D., Yantosca, R.M., Chin, M., 2004. Natural and transboundary pollution influences on sulfate-nitrate-ammonium aerosols in the United States: implications for policy. J. Geophys. Res. Atmos. 109, D15204.
Park, R.J., Jacob, D.J., Kumar, N., Yantosca, R.M., 2006. Regional visibility statistics in the United States: natural and transboundary pollution influences, and implications for the regional haze rule. Atmos. Environ. 40, 5405–5423.
Price, C., Rind, D., 1992. A simple lightning parameterization for calculating global lightning distributions. J. Geophys. Res. Atmos. (1984–2012) 97, 9919–9933.
Qian, Y., Giorgi, F., 2000. Regional climatic effects of anthropogenic aerosols? The case of Southwestern China. Geophys. Res. Lett. 27, 3521–3524.
Qin, S., Shi, G., Chen, L., Wang, B., Zhao, J., Yu, C., Shu, Y., 2010. Long-term variation of aerosol optical depth in China based on meteorological horizontal visibility observations. Chin. J. Atmos. Sci. 34, 449–456.
Rienecker, M.M., Suarez, M.J., Todling, R., Bacmeister, J., Takacs, L., Liu, H.-C., Gu, W., Sienkiewicz, M., Koster, R.D., Gelaro, R., Stajner, I., Nielsen, J.E., 2008. The GEOS-5 data assimilation system—documentation of versions 5.0.1, 5.1.0, and 5.2.0. In: Suarez, M.J. (Ed.), Technical Report Series on Global Modeling and Data Assimilation, p. 118.
Streets, D.G., Bond, T.C., Carmichael, G.R., Fernandes, S.D., Fu, Q., He, D., Klimont, Z., Nelson, S.M., Tsai, N.Y., Wang, M.Q., Woo, J.H., Yarber, K.F., 2003. An inventory of gaseous and primary aerosol emissions in Asia in the year 2000. J. Geophys. Res. Atmos. 108, 8809.
Su, X., Goloub, P., Chiapello, I., Chen, H., Ducos, F., Li, Z., 2010. Aerosol variability over East Asia as seen by POLDER space-borne sensors. J. Geophys. Res. Atmos. (1984–2012) 115, D24215.
Sun, Y., Qi, J., Wang, Z., Fu, P., Jie, L., Yang, T., Yan, Y., 2014. Investigation of the sources and evolution processes of severe haze pollution in Beijing in January 2013. J. Geophys. Res. Atmos. 119, 4380–4398.
van der Werf, G.R., Randerson, J.T., Giglio, L., Collatz, G., Mu, M., Kasibhatla, P.S., Morton, D.C., DeFries, R., Jin, Y.v, van Leeuwen, T.T., 2010. Global fire emissions and the contribution of deforestation, savanna, forest, agricultural, and peat fires (1997–2009). Atmos. Chem. Phys. 10, 11707–11735.
van Donkelaar, A., Martin, R.V., Spurr, R.J., Drury, E., Remer, L.A., Levy, R.C., Wang, J., 2013. Optimal estimation for global ground-level fine particulate matter concentrations. J. Geophys. Res. Atmos. 118, 5621–5636.
Vautard, R., Yiou, P., van Oldenborgh, G.J., 2009. Decline of fog, mist and haze in Europe over the past 30 years. Nat. Geosci. 2, 115–119.
Wang, K.C., Dickinson, R.E., Liang, S.L., 2009. Clear sky visibility has decreased over land globally from 1973 to 2007. Science 323, 1468–1470.
Wang, L., Wang, Y., Xin, J., Li, Z., Wang, X., 2010. Assessment and comparison of three years of terra and aqua MODIS aerosol optical depth retrieval (C005) in Chinese terrestrial regions. Atmos. Res. 97, 229–240.
Wang, Q., Jacob, D.J., Fisher, J.A., Mao, J., Leibensperger, E., Carouge, C., Sager, P.L., Kondo, Y., Jimenez, J., Cubison, M., 2011a. Sources of carbonaceous aerosols and deposited black carbon in the Arctic in winter-spring: implications for radiative forcing. Atmos. Chem. Phys. 11, 12453–12473.
Wang, Y., Xin, J., Li, Z., Wang, S., Wang, P., Hao, W.M., Nordgren, B.L., Chen, H., Wang, L., Sun, Y., 2011b. Seasonal variations in aerosol optical properties over China. J. Geophys. Res. 116, D18209.
Wang, K., Dickinson, R., Su, L., Trenberth, K., 2012. Contrasting trends of mass and optical properties of aerosols over the Northern Hemisphere from 1992 to 2011. Atmos. Chem. Phys. 12, 9387–9398.
Wang, Q., Cao, J., Tao, J., Li, N., Su, X., Chen, L.A., Wang, P., Shen, Z., Liu, S., Dai, W., 2013a. Long-term trends in visibility and at Chengdu, China. PLoS One 8, e68894.
Wang, Z., Peng, Y., Che, H., BAI, A.-j, 2013b. Analyses on spatial and temporal characteristics of AOD in Guanzhong region of Shaanxi Province using long term MODIS data. Plateau Meteor 32, 234–242.
White, W., Roberts, P., 1977. On the nature and origins of visibility-reducing aerosols in the Los Angeles air basin. Atmos. Environ. (1967) 11, 803–812.
Xia, X., Chen, H., Goloub, P., Zong, X., Zhang, W., Wang, P., 2013. Climatological aspects of aerosol optical properties in North China Plain based on ground and satellite remote-sensing data. J. Quant. Spectrosc. Radiat. Transf. 127, 12–23.
Xin, J.Y., Wang, Y.S., Li, Z.Q., Wang, P.C., Hao, W.M., Nordgren, B.L., Wang, S.G., Liu, G.R., Wang, L.L., Wen, T.X., Sun, Y., Hu, B., 2007. Aerosol optical depth (AOD) and Angstrom exponent of aerosols observed by the Chinese sun hazemeter network from August 2004 to September 2005. J. Geophys. Res. Atmos. 112,

D05203.
Yu, X., Zhu, B., Zhang, M., 2009. Seasonal variability of aerosol optical properties over Beijing. Atmos. Environ. 43, 4095–4101.
Zhang, Q., Streets, D.G., Carmichael, G.R., He, K.B., Huo, H., Kannari, A., Klimont, Z., Park, I.S., Reddy, S., Fu, J.S., Chen, D., Duan, L., Lei, Y., Wang, L.T., Yao, Z.L., 2009. Asian emissions in 2006 for the NASA INTEX-B mission. Atmos. Chem. Phys. 9, 5131–5153.
Zhang, L., Liu, L., Zhao, Y., Gong, S., Zhang, X., Henze, D.K., Capps, S.L., Fu, T.-M., Zhang, Q., Wang, Y., 2015. Source attribution of particulate matter pollution over North China with the adjoint method. Environ. Res. Lett. 10, 084011.